Quantitative determination of anti-structured defects applied to alloys of a wide chemical range*

Jing Zhang(张静)†, Zheng Chen(陈铮), Yongxin Wang(王永欣), and Yanli Lu(卢艳丽)

School of Materials Science and Engineering, Northwestern Polytechnical University, Xi'an 710072, China

(Received 15 June 2016; revised manuscript received 10 July 2016; published online 30 September 2016)

Anti-structured defects bridge atom migration among heterogeneous sublattices facilitating diffusion but could also result in the collapse of ordered structure. Component distribution $Ni_{75}Al_xV_{25-x}$ alloys are investigated using a microscopic phase field model to illuminate relations between anti-structured defects and composition, precipitate order, precipitate type, and phase stability. The $Ni_{75}Al_xV_{25-x}$ alloys undergo single Ni_3V (stage I), dual Ni_3Al and Ni_3V (stage II with Ni_3V prior; and stage III with Ni_3Al prior), and single Ni_3Al (stage IV) with enhanced aluminum level. For Ni_3V phase, anti-structured defects (V_{Ni1}, Ni_V, except V_{Ni2}) and substitution defects (Al_{Ni1}, Al_{Ni2}, Al_V) exhibit a positive correlation to aluminum in stage I, the positive trend becomes to negative correlation or smooth during stage II. For Ni_3Al phase, anti-structured defects (Al_{Ni}, Ni_{Al}) and substitution defects (V_{Ni}, V_{Al}) have a positive correlation to aluminum in stage II, but Ni_{Al} goes down since stage III and lasts to stage IV. V_{Ni} and V_{Al} fluctuate when Ni_3Al precipitates prior, but go down drastically in stage IV. Precipitate type conversion of single Ni_3V/dual (Ni_3V+Ni_3Al) affects Ni_3V defects, while dual (Ni_3V+Ni_3Al)/single Ni_3Al has little effect on Ni_3Al defects. Precipitate order swap occurred in the dual phase region affects on Ni_3Al defects but not on Ni_3V.

Keywords: microscopic phase field, anti-structured defects, substitution defect, atom occupancy

PACS: 61.72.J–, 61.50.Ah, 81.30.Mh, 71.15.Pd **DOI:** 10.1088/1674-1056/25/11/116102

1. Introduction

Defects of intermetallic compounds have been widely studied, and will stay active as long as structural materials are in service.[1–5] These defects include dislocations, vacancies, and substitution defects. Dislocations explain that the deformation strengthening vacancies are necessary for atom diffusion, while substitution defects account for solid solution strengthening. However, another kind of defects, named anti-structured defects, have been discussed frequently in semiconductors but scarcely mentioned in structural materials.[6–8] Anti-structured defects are intrinsic defects that strongly rely on temperature and composition. It is not generally distinguished from substitution defects in intermetallic structural materials. An anti-structured atom is usually defined as mistaken atom occupancy. Take face centered cubic A_3B type intermetallic compounds as an example, an A atom resides on the face center (α sublattice) while B is on the corner (β sublattice) in a perfect cube, when A replaces B on the corner an anti-structured defect A_B arises. Similarly, B_A indicates that an anti-structured atom B replaces the host atom A on α sublattice (face center), graphically demonstrated in Fig. 1. Experimental observation and theoretical computation have manifested that anti-structured defects are considerably greater than vacancies.[9,10] Anti-structured defects participate in atom diffusion in many ways, for example, triple-defect mechanism,[11,12] anti-structure bridge mechanism,[13–15] six-jump cycle mechanism,[16,17] divacancy mechanism,[18–20] and intrasublattice mechanism.[21–23] On the other hand, too many anti-structured defects will result in structure collapse and catastrophic mechanical failure.

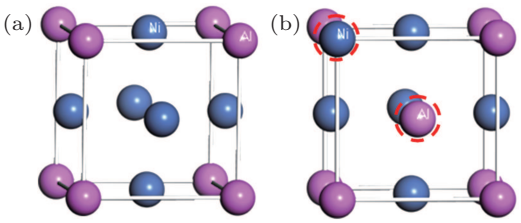


Fig. 1. (color online) Schematic representation of $L1_2$-Ni_3Al: (a) perfect structure, (b) an example of anti-structured defects Ni_{Al} and Al_{Ni} (gray dots are Ni atoms, purple dots are Al atoms).

Diffusion by vacancy migration is generally accepted in the tradition. Theoretical computation verified the overwhelming superiority of anti-structured defects in intermetallic compounds, therefore, the idea that atom diffuses via anti-structured defects arises.[13,17,20] Take the $L1_2$-Ni_3Al phase as an example, one nickel atom is accompanied by eight nickel atoms and four aluminum atoms, therefore, a nickel atom can migrate by exchanging with the neighbor nickel (α sublattice) without disturbing the β sublattice. An aluminum atom has twelve direct bonded nickel atoms as neighbors, thus, it is un-

*Project supported by the Natural Science Basic Research Plan in Shaanxi Province of China (Grant No. 2016JQ5014), the Fundamental Research Funds for the Central Universities, China (Grant No. 3102014JCQ01024), the Research Fund of the State Key Laboratory of Solidification Processing (NWPU), China (Grant No. 114-QP-2014), the Specialized Research Fund for the Doctoral Program of Higher Education of China (Grant No. 20136102120021), and the National Natural Science Foundation of China (Grant Nos. 51474716 and 51475378).

†Corresponding author. E-mail: Jingzhang@nwpu.edu.cn

© 2016 Chinese Physical Society and IOP Publishing Ltd

favorable for it moving exclusively through the β sublattice, it has to migrate through the α sublattice via anti-structured defects Al_{Ni}. As a matter of fact, even a nickel atom also migrates through α and β sublattices with the participation of anti-structured defects Ni_{Al}.[25,26]

Ternary Ni–Al–V alloy, having fcc-derived $L1_2$-Ni_3Al and $D0_{22}$-Ni_3V phases precipitate competitively, exhibits prominent performance such as outstanding high-temperature strength, high structure stability, and good oxidation resistance ascribing to the abnormal stress effect. Ni_3Al phase can hold $L1_2$ configuration until the melting point because of the low diffusivity due to the geometry close packing structure. Ni_3V phase with $D0_{22}$ configuration is unstable when aluminum is added, its β sublattice is prone to be occupied by aluminum addition, and leads to the Ni_3(Al, V) phase transforms from $D0_{22}$ to $L1_2$. Ni_3(Al, V) compound may display $L1_2$ structure or $D0_{22}$ structure while most experimental observation and theoretical computation favor $L1_2$ other than $D0_{22}$.[1,2] This intrinsic property of $D0_{22}$ structure can also account for drastic Ni_3V reduction when the aluminum composition is slightly enhanced. Both Ni_3Al and Ni_3V phases are characterized by low vacancies but concentrated anti-structured defects.[26,27] Many prominent properties are related to the thermodynamic equilibrium anti-structured defects linking to chemical composition. The relation between anti-structured defects and the composition is clarified by the manipulating chemical ratio of Al/V in $Ni_{75}Al_xV_{25-x}$ alloys in this study. For such an $L1_2$–$D0_{22}$ competitive precipitation system the relation is more than a simple issue related to the composition but to the precipitate type and the order with the composition varying.

2. Equation of motion

The microscopic phase field model is generally used to describe the microstructure evolution and the related quantitative prediction.[28–31] It characterizes the phase transition and the morphology evolution using single sublattice atom occupancy probabilities $P_A(r,t)$, $P_B(r,t)$, and $P_C(r,t)$, for a ternary system. Here, $P_A(r,t)$, $P_B(r,t)$, and $P_C(r,t)$ represent the single sublattice atom occupancy probabilities of elements A, B, and C at a given time t and sublattice r, respectively. Ignore the vacancy effect and simplify the model, these three atom occupancy probabilities fulfil $P_A(r,t)+P_B(r,t)+P_C(r,t)=1$ with only two independent items on each sublattice. Suppose A and B are the two independent variables, the Langevin-type dynamic equation is given by[32]

$$\begin{cases} \dfrac{\mathrm{d}P_A(r,t)}{\mathrm{d}t}=\dfrac{1}{k_BT}\sum\limits_{r}^{\prime}\left[L_{AA}(r-r')\dfrac{\partial F}{\partial P_A(r',t)}+L_{AB}(r-r')\dfrac{\partial F}{\partial P_B(r',t)}\right]+\xi(r,t), \\ \dfrac{\mathrm{d}P_B(r,t)}{\mathrm{d}t}=\dfrac{1}{k_BT}\sum\limits_{r}^{\prime}\left[L_{BA}(r-r')\dfrac{\partial F}{\partial P_A(r',t)}+L_{BB}(r-r')\dfrac{\partial F}{\partial P_B(r',t)}\right]+\xi(r,t), \end{cases} \tag{1}$$

where $L(r-r')$ is a constant related to the exchange probability of a pair of atoms at r and r' per unit time; T is the absolute temperature; k_B is the Boltzmann constant; $\xi(r,t)$is a thermal noise governed by fluctuation-dissipation theorem to simulate the thermal fluctuation; F is the total free energy given by the following equation under the mean-field approximation:

$$\begin{aligned} F = & -\frac{1}{2}\sum_{r}\sum_{r'}\left[(-V_{AB}(r-r')+V_{BC}(r-r')\right. \\ & +V_{AC}(r-r'))P_A(r)P_B(r')+V_{AC}(r-r')P_A(r)P_A(r') \\ & \left.+V_{BC}(r-r')P_B(r)P_B(r')\right] \\ & +k_BT\sum_{r'}\left[P_A(r)\ln(P_A(r))+P_B(r)\ln(P_B(r))\right] \\ & +(1-P_A(r,t)-P_B(r,t))\ln(1-P_A(r,t)-P_B(r,t)), \end{aligned} \tag{2}$$

where $V_{ab}(r-r\prime)$ is the interaction energy between components a (a is A, B or C) at sublattice r and b (b is A, B or C) at sublattice r'. Considering all the likely atom migration and the arrangement of the three components, a fourth-nearest neighbor interaction energy model is introduced to describe the free energy. The V_{ab}^1,V_{ab}^2,V_{ab}^3,V_{ab}^4 are respectively, the first-, second-, third-, and fourth-nearest neighbors with an effective interchange interaction energy between components a and b.

In this study concerning Ni–Al–V alloy, we use the following interaction parameters (meV/atom):[32]

Nickel and aluminum interaction: $V_1=122.30$, $V_2=6.0$, $V_3=16.58$, and $V_4=-6.82$;

Nickel and vanadium interaction: $V_1=107.2$, $V_2=32.0$, $V_3=-9.6$, and $V_4=12.8$;

Aluminum and vanadium interaction: $V_1=40.0$, $V_2=-30.0$, $V_3=-80.0$, and $V_4=0.0$. The interaction energy can be written as

$$\begin{aligned} V_{ab}(k) = & 4V_{ab}^1(\cos\pi h\cos\pi k+\cos\pi h\cos\pi l+\cos\pi k\cos\pi l) \\ & +2V_{ab}^2(\cos 2\pi h+\cos 2\pi k+\cos 2\pi l) \\ & +8V_{ab}^3\big(\cos 2\pi h\cos\pi k\cos\pi l \\ & +\cos\pi h\cos 2\pi l\cos\pi l \\ & +\cos\pi k\cos\pi l\cos 2\pi l\big)+4V_{ab}^4\big(\cos 2\pi h\cos 2\pi k \\ & +\cos 2\pi h\cos 2\pi l+\cos 2\pi k\cos 2\pi l\big). \end{aligned} \tag{3}$$

It is advantageous in quantitatively describing the atom distribution using atom occupancy probabilities of P_A, P_B, and P_C. We capitalize on this advantage to explore atom occupancy-composition relation involving atom rearrangement and phase transition.

3. Results and discussion

Computation proceeds on a 128×128 matrix with periodic boundary condition applied along both Cartesian axes. The $Ni_{75}Al_xV_{25-x}$ alloys contain 75 at.% nickel and total 25 at.% aluminum and vanadium. Aluminum composition is enhanced consecutively from 1 at.% Al to 20 at.% Al with a concentration gradient of 1%. Atom occupancy probabilities of nickel, aluminum and vanadium are checked on each 128×128 site for these alloys.

3.1. Precipitate order and precipitate phases

Precipitated phases Ni_3V and Ni_3Al evolve in a way "single Ni_3V phase $\rightarrow$ dual Ni_3Al and prior Ni_3V phase $\rightarrow$dual Ni_3V and prior Ni_3Al phase $\rightarrow$single Ni_3Al phase" with the enhanced aluminum composition, a typical example of such a "microstructure-chemical composition relation" is shown in Fig. 2 for $Ni_{75}Al_xV_{25-x}$ alloys aging at 1150 K. In detail, the whole process can be divided into four stages by the precipitate order and phases as follows.

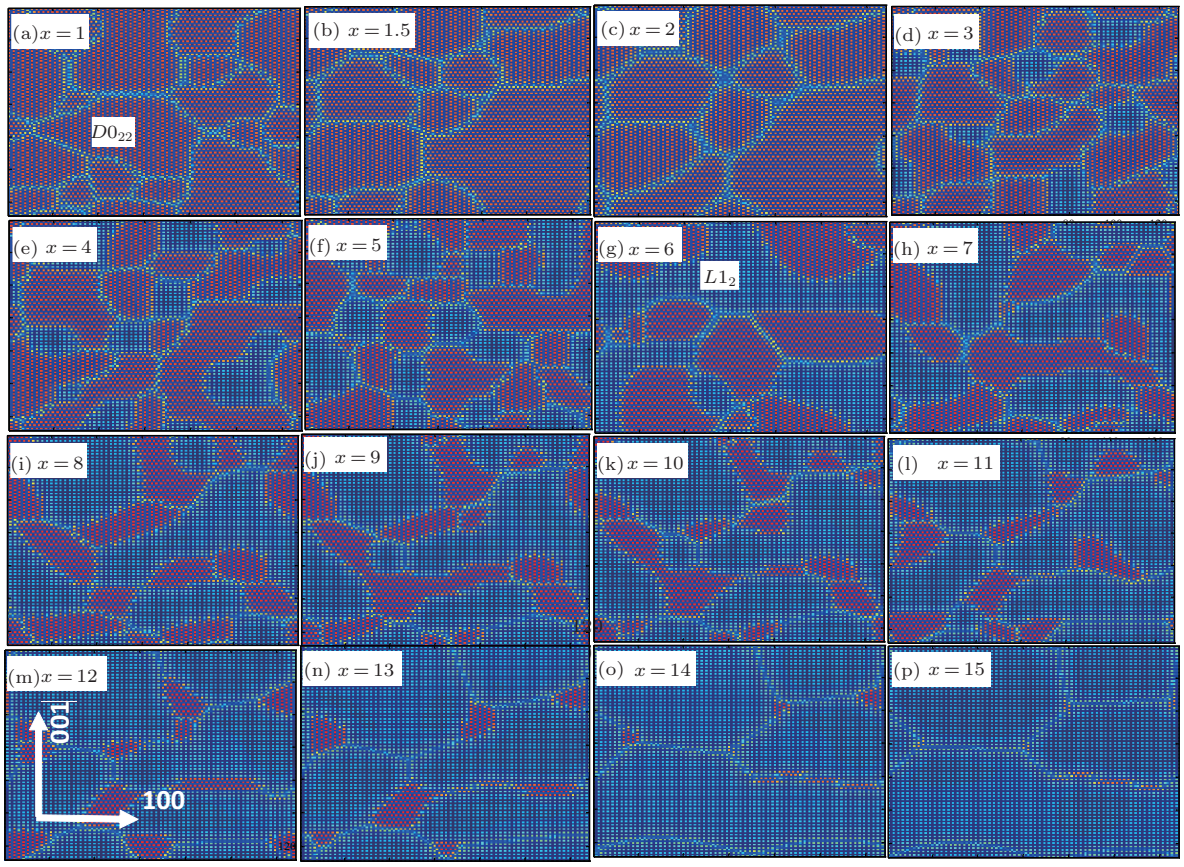


Fig. 2. (color online) Microstructure evolution with the enhanced aluminum composition for $Ni_{75}Al_xV_{25-x}$ alloys aging at 1150 K. (a) $x = 1$, (b) $x = 1.5$, (c) $x = 2$, (d) $x = 3$, (e) $x = 4$, (f) $x = 5$, (g) $x = 6$, (h) $x = 7$, (i) $x = 8$, (j) $x = 9$, (k) $x = 10$, (l) $x = 11$, (m) $x = 12$, (n) $x = 13$, (o) $x = 14$, and (p) $x = 15$.

Stage I: at.% Al$<$ 2 at.%, single Ni_3V phase region;

Stage II: 2 at.% $<$ at.% Al$<$ 5 at.%, dual Ni_3Al and prior Ni_3V phase region with Ni_3V precipitates prior to Ni_3Al;

Stage III: 5 at.% $<$ at.% Al$<$ 13 at.%, dual Ni_3V and prior Ni_3Al phase region with Ni_3Al precipitates prior to Ni_3V;

Stage IV: at.% Al$>$13 at.%, single Ni_3Al phase region.

The four stages are graphically demonstrated in Fig. 3.

3.2. Anti-structured defects of Ni_3Al

Figure 4 demonstrates the atom occupancy–composition relations of nickel, aluminum, and vanadium on α sublattice since stage II where the Ni_3Al phase starts to precipitate. In stage II, the atom occupancies of three components proceed as host Ni_{Ni} downs, anti-structured defects Al_{Ni} and substitution defects V_{Ni} increase with the increase of the aluminum composition. The precipitate order swaps since stage III where Ni_3Al phases start to precipitate prior to Ni_3V. Atom occupancies of Ni_{Ni} and V_{Ni} fluctuate in a narrow range while that of Al_{Ni} increases slightly. Ni_3V phases precipitate no more since stage IV, the atom occupancies of Ni_{Ni} and Al_{Ni} increase while that of V_{Ni} decreases. These trends last to 18 at.% Al.

Atom occupancy–composition relation on β sublattice is demonstrated in Fig. 5. It is worth mentioning that the scale of y axis in Fig. 5 is ten times larger than that in Fig. 4, which indicates more drastic atom occupancy fluctuation on the β sublattice than that on the α sublattice. In stage II, the atom occupancy of host atom Al_{Al} decreases while those of anti-structured defects Ni_{Al}

and substitution defects V_{Al} increase with the increase of the aluminum composition. In stage III, the atom occupancy of Al_{Al} increases while that of Ni_{Al} decreases drastically, the atom occupancy of V_{Al} becomes stable. Ni_3V phases fade since stage IV resulting in the atom occupancy of host Al_{Al} increasing but those of Ni_{Al} and V_{Al} decreasing till 18 at.% Al.

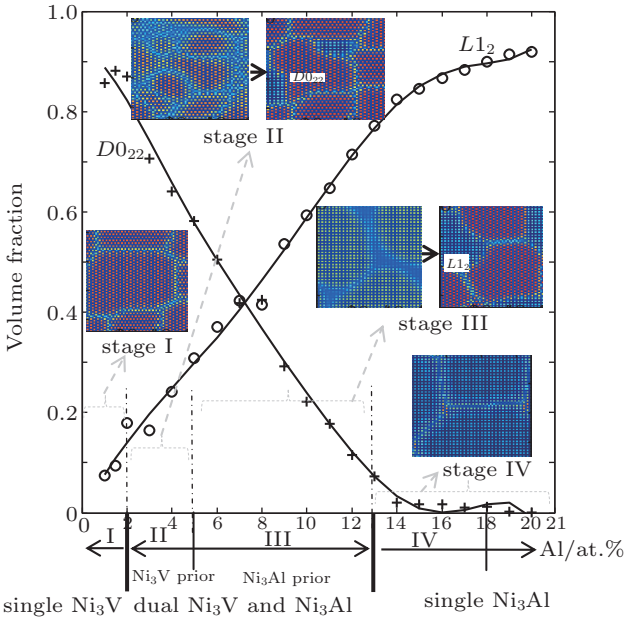


Fig. 3. (color online) Volume fraction–composition relation and microstructure division.

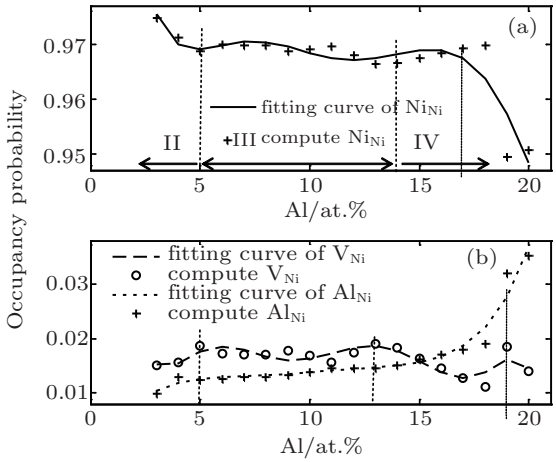


Fig. 4. Atom occupancy–composition relation of Ni_3Al α sublattice. (a) Ni_{Ni}, (b) V_{Ni} and Al_{Ni}.

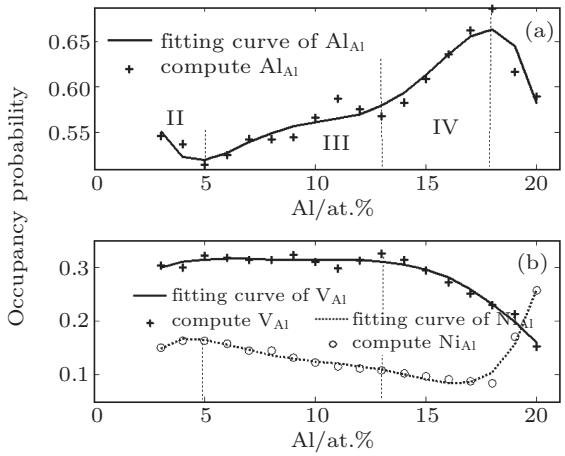


Fig. 5. Atom occupancy–composition relation of Ni_3Al β sublattice. (a) Al_{Al}, (b) V_{Al} and Ni_{Al}.

As stated above, anti-structured defects as well as other atoms show a certain composition correlation depending on the precipitate order and precipitated phases. First, the α sublattice is predominated by the host nickel with little anti-structured defects Al_{Ni} and substitution defects V_{Ni}. Al_{Ni} has a constant positive correlation with an enhanced aluminum level, precipitate order swap does not affect its occupancy while precipitated phase conversion of "dual Ni_3V and Ni_3Al/single Ni_3Al" does as the rising trend lasts to a single Ni_3Al region. The atom occupancy of substitution defects V_{Ni} fluctuates in a small range, and their composition correlation varies when the precipitate order swaps at 5 at.%Al or Ni_3V phases disappear at 13 at.% Al. Second, compared with the α sublattice, the β sublattice accommodates more alien atoms, the atom occupancy of anti-structured defects Ni_{Al} is almost ten times higher than that of Al_{Ni}. Ni_{Al} and host Al_{Al} present just opposite composition correlations, and strongly depend on the precipitate order and precipitated phases. Substitution defects V_{Al} take almost one third of that of the β sublattice, they are not affected by the precipitate order but by the disappearance of Ni_3V.

It is easy to understand the positive composition correlation of anti-structured defects Al_{Ni} and host Al_{Al} in stages III and IV, as concentrated aluminum-concentration concentrated aluminum-occupancy. The enhanced aluminum composition means lessened vanadium, however, the vanadium occupancy is comparatively smooth and does not lessen seriously over stages II, III and IV. Once Ni_3Al phases start to precipitate, their volume fraction increases fast, thus, the average nickel and aluminum atom assigned to each $L1_2$ cube lessens, that is, the atom occupancies of host Ni_{Ni} and Al_{Al} decrease, consequently, the spared sublattice replaced by anti-structured or substitution defects is enhanced in stage II. Ni_3Al precipitates prior to Ni_3V since stage III, their volume fraction keeps increasing and holds a high Ni_{Ni} occupancy, which demands vast nickel, thus, nickel atoms that serve as anti-structured defects Ni_{Al} reduce. Ni_3V phases fade since stage IV, Ni_3Al phases coalesce to a larger size, the atom composition correlation is simply ascribed to the Ni_3Al volume and the aluminum composition. Ni_3V volume fraction decreases fast in the whole process, which releases a large amount of vanadium. The released vanadium weighs more than the lessened one, thus, the surplus one is accommodated by Ni_3Al and comes to a rough balance, that is why the vanadium occupancy fluctuates with the sharply increased Ni_3Al over stages II, III, and IV.

3.3. Anti-structured defects of Ni_3V phase

The $Ni_3V\alpha$ sublattice is subdivided into two other sublattices, a Ni_1 sublattice, and a Ni_2 sublattice according to their coordination sphere differences. Figure 6 demonstrates the atom occupancy–composition relation on the α (Ni_1 and Ni_2) sublattice. The atom occupancy of host Ni_{Ni1} decreases while that of Ni_{NiII} increases in stage I, the gap between Ni_{Ni1} and Ni_{Ni2} gets narrow crossing stage I and stage II but widens gradually crossing stage II and stage III. The atom occupancy of Ni_{Ni1} fluctuates in a narrow range while that of Ni_{Ni2} consistently decreases from stage II to stage III. The occupancy gap between substitution defects Al_{Ni1} and Al_{Ni2} is quite wide with super site preference on the Ni_1 sublattice, and there is no obvious composition correlation except Al_{Ni1}. Anti-structured vanadium has overwhelming site preference on the Ni_2 sublattice. The atom occupancy of V_{Ni1} keeps increasing subtly while that of V_{Ni2} decreases in stage I but increases in stages II and III.

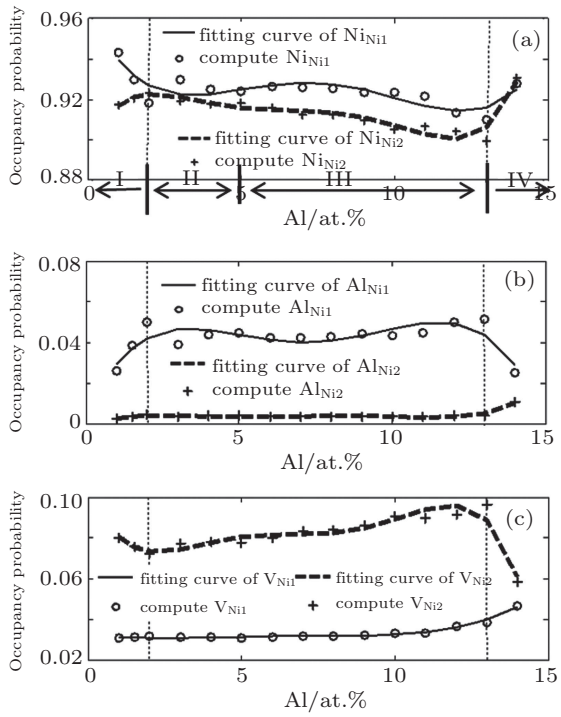


Fig. 6. Atom occupancy–composition relation of Ni_3V α sublattice. (a) Ni_{Ni1} and Ni_{Ni2}, (b) Al_{Ni1} and Al_{Ni2}, and (c) V_{Ni1} and V_{Ni2}.

Atom occupancy–composition relation on the β sublattice is presented in Fig. 7. The atom occupancy of host atom V_V decreases in stage I, but increases crossing stages II and III. The atom occupancy of anti-structured defects Ni_V exhibits an opposite trend to V_V. The atom occupancy of substitution defects Al_V increases slightly in stage I but shows no evident composition correlation in stages II and III.

There is an occupancy difference in the two nickel sublattices, that is, the Ni1 sublattice accommodates a few anti-structured defects V_{Ni1} and more substitution defects Al_{Ni1} while the Ni2 sublattice accommodates more anti-structured defects V_{Ni2} and a few substitution defects Al_{Ni2}. This occupancy difference is ascribed to their coordination sphere difference but the exact mechanism is unknown. Compared with the α sublattice, the β sublattice is easier to be replaced by alien atoms anti-structured defects Ni_V dominate on the β sublattice with very little substitution defects Al_V.

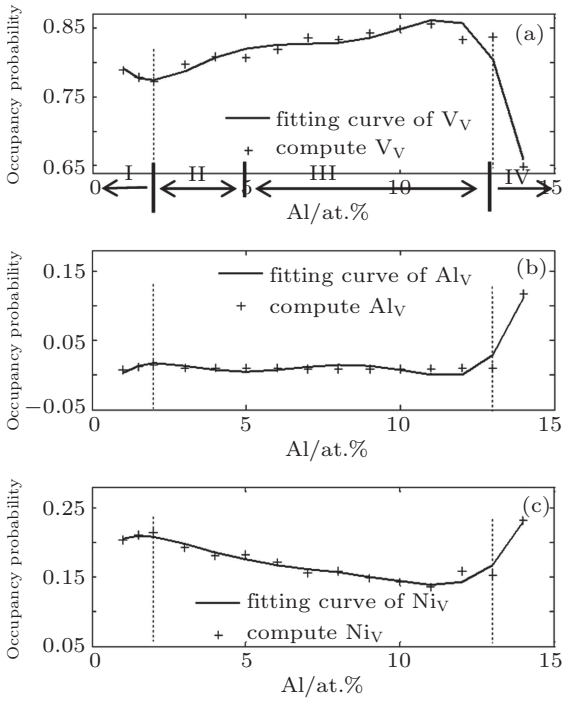


Fig. 7. Atom occupancy–composition relation of Ni_3V β sublattice. (a) V_V, (b) Al_V, and (c) Ni_V.

The precipitate order swap at 5 at.%Al has no obvious effect on the atom occupancy, while precipitate phase conversion of "single Ni_3V/dual Ni_3Al and Ni_3V" since 2 at.%Al does. It is easy to understand that the atom occupancies of substitution defects Al_{Ni1}, Al_{Ni2}, and Al_V increase and that of anti-structured defects V_{Ni2} decreases in stage I as aluminum is enhanced while vanadium is lessened. Anti-structured defects V_{Ni1} and V_{Ni2} have a positive composition correlation, anti-structured defects Ni_V have negative one while aluminum occupancy fluctuates in a small range over stages II and III. As discussed in the last section, the Ni_3V volume fraction goes down fast and releases a large amount of vanadium which is used to compensate the $Ni_3V\beta$ sublattice, dissolve into the Ni_3V α sublattice, and be accommodated by the Ni_3Al β sublattice, that is why the atom occupancies of V_{Ni1}, V_{Ni2}, and V_V increase. On the $Ni_3V\beta$ sublattice, the increase of vanadium (V_V) cause nickle occupancy (Ni_V) down. Similar to the role of vanadium on Ni_3Al, the atom occupancies of substitution defects Al_{Ni1}, Al_{Ni2}, and Al_V on Ni_3V fluctuate due to the rough balance.

4. Conclusions

Microscopic phase field computation is proceeded on a 128×128 matrix to investigate anti-structured defects. A series of Ni–Al–V samples with aluminum composition ranging from 1 at.% Al to 20 at.% Al are examined. Four stages are summarized according to the precipitate order and precipitated phases. Precipitated phases converse at separate 2 at.% Al and 13 at.% Al with dual Ni_3Al and Ni_3V in the middle, single Ni_3V on the heading, and single Ni_3Al on the tail. The precipitate order swaps at 5 at.% Al, which Ni_3V precipitates prior with insufficient aluminum composition and Ni_3Al precipitates prior since 5 at.% Al.

Anti-structured defects Ni_{Al} dominate in Ni_3Al phases while Al_{Ni} are minor. The Ni_3Al β sublattice accommodates a large amount of anti-structured defects Ni_{Al} and substitution defects V_{Al}. All defects show positive composition correlations in stage II. The atom occupancy of Al_{Ni} goes up slightly while that of Ni_{Al} decreases since 5 at.%Al, this trend lasts to the single Ni_3Al region. The atom occupancies of substitution defects V_{Ni} and V_{Al} fluctuate in a small range over stage III, and decrease drastically from a single Ni_3Al region.

The Ni_3V β sublattice is easier to be replaced by defects than their α sublattice. Both anti-structured defects and substitution defects have a positive composition correlation except V_{Ni2} in the single Ni_3V region; this positive trend inverses or becomes smooth since the Ni_3Al phases start to precipitate at 2 at.%Al. The atom occupancy of anti-structured defects Ni_V keeps decreasing while that of substitution defects V_{Ni2} keeps increasing over the whole dual phases region, the precipitate order swap at 5 at.%Al does not have much effect on the atomic occupancy.

In a word, the precipitate order swap effects Ni_3Al defects while the precipitated phase conversion effects Ni_3V defects. No matter what Ni_3Al phases or Ni_3V phases are, their β sublattices are easier to be replaced by anti-structured defects or substitution defects.

References

[1] Ding H, Medasani B, Chen W, Persson K A, Haranczyk M and Asta M 2015 *Comput. Phys. Commun.* **193** 118
[2] Bai J, Wang X S, Zu Q R, Zhao X and Zuo L 2016 *Acta Phys. Sin.* **65** 96103 (in Chinese)
[3] Yu S, Wang C Y and Yu T 2007 *Acta Phys. Sin.* **56** 3212 (in Chinese)
[4] Groïhagen K, Ågren J and Odeń M 2015 *Scripta Mater.* **95** 42
[5] Li Y S, Chen X L, Xu F and Du Y L 2011 *Chin. Phys. Lett.* **28** 106601
[6] Zawadzki P, Zakutayev A and Lany S 2015 *Phys. Rev. B* **92** 201204
[7] Devaraju M K, Truong Q D, Hyodo H, Sasaki Y and Honma I 2015 *Sci. Rep.* **51** 11041
[8] Song J X, Yang Y T, Guo L X, Wang P and Zhang Z Y 2012 *Acta Phys. Sin.* **61** 237301 (in Chinese)
[9] Zhang Z, Bai B, Peng H and Guo H 2015 *Mater. Design* **88** 667
[10] Tingaud D and Besson R 2014 *Intermetallics* **45** 38
[11] Breuer J, Sommer F and Mittemeijer E J 2002 *Phil. Mag. A* **82** 479
[12] Frank S, Divinski S V, Södervall U and Herzig C 2001 *Acta Mater.* **49** 1399
[13] Kao C R and Chang Y A 1993 *Intermetallics* **1** 237
[14] Kurzawski Ł and Malarz K 2012 *Rep. Math. Phys.* **70** 163
[15] Herzig C and Divinski S 2004 *Intermetallics* **12** 993
[16] Drautz R and Fähnle M 1999 *Acta Mater.* **47** 2437
[17] Belova I V and Murch G E 2002 *Philos. Mag. A* **82** 269
[18] Korzhavyi P A, Ruban A V, Lozovoi A Y, Vekilov Y K, Abrikosov I A and Johansson B 2000 *Phys. Rev. B* **61** 6003
[19] Bocquet J L 2015 *Philos. Mag.* **95** 394
[20] Du Y, Chang Y A, Huang B, Gong W, Jin Z, Xu H, Yuan Z, Liu Y and Xie F Y 2003 *Mater. Sci. Eng. A* **363** 140
[21] Gopal P and Srinivasan S G 2012 *Phys. Rev. B* **86** 014112
[22] Duan J 2007 *J. Phys.: Condens. Matter* **19** 086217
[23] Murch G E and Belova I V 2001 *J. Mater. Process. Tech.* **118** 82
[24] Marteau L, Pareige C and Blavette D 2001 *J. Microsc.* **204** 247
[25] Wang J S 1998 *Acta Mater.* **46** 2663
[26] Ruban A V, Popov V A, Portnoi V K and Bogdanov V I 2014 *Philos. Mag.* **94** 20
[27] Wu Q and Li S 2012 *Comp. Mater. Sci.* **53** 436
[28] Kundin J, Wang P, Emmerich H and Schimid-Fetzer R 2014 *Eur. Phys. J. Spec. Top.* **223** 567
[29] Ta N, Zhang L, Tang Y, Chen W and Du Y 2015 *Surf Coat. Tech.* **261** 364
[30] Gránásy L, Rátkai L, Szállás A, Korbuly B, Tóth G I, Környei L and Pusztai T 2014 *Metall. Mater. Trans. A* **45** 1694
[31] Yang T, Zhang J, Long J, Long Q H and Chen Z 2014 *Chin. Phys. B* **23** 088109
[32] Poduri R and Chen L Q 1998 *Acta Mater.* **46** 1719